A New Suite of Allelic Exchange Vectors for the Scarless Modification of Proteobacterial Genomes

Jacob E. Lazarus[1,2], Alyson R. Warr[2,3], Carole J. Kuehl[2,3], Rachel T. Giorgio[2,3], Brigid M. Davis[2,3], Matthew K. Waldor[2,3,4,*]

[1] Division of Infectious Digmseases, Massachusetts General Hospital, Boston, MA, USA

[2] Department of Microbiology, Harvard Medical School, Boston, MA, USA

[3] Division of Infectious Diseases, Brigham and Women's Hospital, Boston, MA, USA

[4] Howard Hughes Medical Institute, Boston, MA, USA

[*] Correspondence to MWALDOR@research.bwh.harvard.edu

Running Title: New Allelic Exchange Vectors for Proteobacteria

Keywords: Allelic exchange, toxin-antitoxin, Type VI toxin, *sacB*, *rhaS*, rhamnose induction, *amilCP*, *tsPurple*, *Serratia marcescens, Shigella flexneri, ampC, ampD, amiD*, peptidoglycan, amidohydrolase, beta-lactamase, antibiotic resistance

Abstract

Despite the advent of new techniques for genetic engineering of bacteria, allelic exchange through homologous recombination remains an important tool for genetic analysis. Currently, *sacB*-based vector systems are often used for allelic exchange, but counter-selection escape, which prevents isolation of cells with the desired mutation, limits its utility. To circumvent this limitation, we engineered a series of “pTOX” allelic exchange vectors. Each plasmid encodes one of a set of inducible toxins, chosen for their potential utility in a wide range of medically important Proteobacteria. A codon-optimized *rhaS* transcriptional activator with a strong synthetic ribosome binding site enables tight toxin induction even in organisms lacking an endogenous rhamnose regulon. Expression of the blue *amilCP* or magenta *tsPurple* non-fluorescent chromoproteins facilitates monitoring of successful single- and double-crossover events using these vectors. The versatility of these vectors was demonstrated by deleting genes in *Serratia marcescens*, *Escherichia coli* O157:H7, *Enterobacter cloacae*, and *Shigella flexneri*. Finally, pTOX was used to characterize the impact of disruption of all combinations of the 3 orthologous *S. marcescens* peptidoglycan amidohydrolases on chromosomal *ampC* beta-lactamase activity and corresponding beta-lactam antibiotic resistance. Mutation of multiple amidohydrolases was necessary for high level *ampC* derepression and beta-lactam resistance. These data suggest why beta-lactam resistance may emerge during treatment less frequently in *S. marcescens* than in other AmpC-producing pathogens like *E. cloacae.* Collectively, our findings suggest that the pTOX vectors should be broadly useful for genetic engineering of Gram-negative bacteria.

40 **Importance**

41 Targeted modification of bacterial genomes is critical for genetic analyses of microorganisms.
42 Allelic exchange is a technique that relies on homologous recombination to substitute native loci for
43 engineered sequences. However, current allelic exchange vectors often enable only weak
44 selection for successful homologous recombination. We developed a suite of new allelic exchange
45 vectors, pTOX, which were validated in several medically important Proteobacteria. They encode
46 visible non-fluorescent chromoproteins that enable easy identification of colonies bearing
47 integrated vector, and permit stringent selection for the second step of homologous recombination,
48 yielding modified loci. We demonstrate the utility of these vectors by using them to investigate the
49 effect of inactivation of *Serratia marcescens* peptidoglycan amidohydrolases on beta-lactam
50 antibiotic resistance.

Introduction

The ever-increasing availability of bacterial genome sequence data has driven the demand for widely applicable and facile techniques enabling site-specific targeted mutagenesis. In general, such techniques can be divided into those that rely on exogenous enzymes versus those that depend exclusively on endogenous enzymes. Examples of methods in the former category include those utilizing the Lambda Red recombinase ("recombineering" (1)), those employing clustered regularly interspaced short palindromic repeat (CRISPR)/Cas9 systems (2), or a combination of the two (3, 4). These systems can be fast and reliable, but often require organism-specific modifications, rely on efficient transformation, and can leave genetic scars or result in off-target mutations.

In contrast, "allelic exchange" utilizes endogenous homologous recombination enzymes to facilitate the replacement of a native genomic region with a foreign sequence of interest. This is a versatile technique that can routinely yield mutations ranging from kilobase-scale deletions or insertions to the generation of precise point mutations. The early allele exchange vectors resulted in antibiotic-marked strains (5, 6); subsequent advances using counter-selectable cassettes allowed the generation of truly scarless, unmarked mutant strains. However, many genes used in counter-selection strategies (*e.g. rpsL*, *pheS, thyA, ccdB)* require a specific host genotype, limiting their widespread utility (7). Background-independent counter-selection strategies utilizing *tetAR* (8), *sacB* (9), or a combination of the two (10) are valuable but often require considerable optimization. Moreover, counter-selection escape, where the integrated allelic exchange vector remains lodged in the genome, preventing isolation of the desired mutant, remains common with such schemes even after optimization. This has been a key technical obstacle limiting wider use of allelic exchange.

Recently, a powerful negative selection system using inducible toxins derived from toxin-antitoxin systems or from Type VI secreted effector-toxins was developed for use with recombineering (11). Here, we repurpose these toxins for use in allelic exchange and engineer a counter-selection escape surveillance system using visible chromoproteins derived from the *Acropora millepora* coral. We demonstrate the utility of these new allele exchange vectors, designated “pTOX,” in multiple medically important Proteobacteria. These vectors were used to systematically delete all combinations of the three peptidoglycan hydrolases in *Serratia marcescens* to characterize their contributions to beta-lactam antibiotic resistance.

Results

Engineering and testing of pTOX vectors

The motivation for this work arose from our difficulties adapting common genetic tools for use in *Serratia marcescens,* an Enterobacteria that is a common cause of healthcare-associated urinary tract infections, pneumonia, and bacteremia (12). While chemical- and electro-transformation is possible in many *S. marcescens* strains (13, 14), it is often cumbersome and inefficient, which reduces the utility of Lambda red recombinase- and CRISPR/Cas9-based systems for genetic manipulation. Because of this, we sought to construct a conjugatable allelic exchange vector for *S. marcescens* that would be widely useful.

Our set of new vectors (the pTOX vectors) is derived from pDS132, a *sacB*-based suicide plasmid that contains the conditional (π-dependent) R6K origin of replication (15). The *sacB* cassette was replaced with a rhamnose-inducible toxin obtained from the pSLC vector series (11) (Fig 1A). Reasoning that a given toxin would be most useful in a strain that did not encode a chromosomal copy of that same toxin (and presumably the corresponding antitoxin or immunity protein), we identified a minimal set of three toxins (*yhaV, mqsR,* and *tse2*), of which at least one should be effective in the majority of medically important proteobacteria (Fig S1). Additional steps in the

construction of this set of vectors included: 1) Introduction of a codon-optimized *rhaS* transcriptional activator (16) with a strong synthetic ribosome binding site (17) to enable use of the well-characterized and stringent rhamnose-inducible system for toxin activation (18) even in strains that lack a rhamnose regulon; 2) introduction of a strong forward transcriptional terminator upstream of the multiple cloning site, minimizing read-through into the multiple cloning site and facilitating the manipulation of toxic genes; and 3) introduction of a greatly expanded polylinker region (19) (Fig 1A) to facilitate insertion of new sequences into the vectors. Two versions of this set of plasmids, encoding either chloramphenicol or gentamicin resistance, were created (Supp Table 2). All molecular cloning was performed in the presence of glucose, which inhibits toxin production through catabolite repression.

The utility of each of the three toxins was validated in *S. marcescens* ATCC 13880, which lacks *rhaS* and endogenous versions of the 3 toxins. First, a region homologous to the targeted chromosomal locus was inserted into the pTOX multiple cloning site (see the Methods for more detail and Fig 1B for a schematic). Next, conjugation was used to introduce pTOX derivatives into *S. marcescens.* Single cross-over merodiploids were selected on the appropriate antibiotic. To assess the utility of the heterologous *rhaS*, we then compared the growth of merodiploids to wild-type *S. marcescens* in either glucose- or rhamnose-containing media. Toxin-containing merodiploids grown in glucose-containing media grew indistinguishably from wild-type, while growth in rhamnose-containing media was undetectable (Fig 2). These observations reveal that *yhaV*, *mqsR*, and *tse2* enable robust growth inhibition in *S. marcescens* and that the exogenous *rhaS* is sufficient for stringent control of their expression.

A limitation of the *sacB* counter-selection system is the occasional outgrowth of merodiploids that have either mutated the *sacB* gene or acquired resistance to its product (9). Such counter-selection escape can confound isolation of double-crossover events. To assess whether counter-

selection escape also confounds *yhaV*-, *mqsR*-, or *tse2*-based selections, we randomly selected 23 colonies representing putative double-crossovers (based on growth in the presence of rhamnose) from 3 independent experiments for each of the three toxin-vectors. All 207 colonies screened were chloramphenicol sensitive and lacked pTOX vector sequences by PCR (Table 1 and Fig S2). These observations suggest that selection mediated by the 3 toxins is potent and that the frequency of counter selection escape is very low.

Utility of pTOX vectors in diverse pathogens

To investigate the versatility of the pTOX vectors, we tested their capacity to mediate diverse allele replacements, beginning with the *S. marcescens hexS* locus. *S. marcescens* ATCC 13880, like many isolates of this opportunistic pathogen, produces the red prodigiosin pigment; however, production is only robust at reduced temperatures, due to relief of repression mediated by the negative regulator *hexS* (20). A pTOX derivative encoding sequences flanking *hexS* was used to delete this regulator from the *S. marcescens* chromosome, resulting in prodigiosin hyperproduction even at 37ºC (Fig 3A). Subsequently, we have replaced more than 20 loci in *S. marcescens* using pTOX1, pTOX2, and pTOX3 (Supplemental Table 2). All attempts have been successful, though like other allelic exchange methods, the ratio of wild-type to mutant double-crossovers can vary from balanced to skewed.

We also tested the utility of the pTOX vectors in 3 additional Gram-negative pathogens. *Escherichia coli* O157:H7 (EHEC) is an important cause of foodborne diarrhea as well as a systemic microangiopathy which can lead to hemolysis and renal failure. A pTOX3 derivative was used to delete *lacZ,* which produces a beta-galactosidase that enables wild-type EHEC to ferment lactose. As seen in Fig 3B, deletion of EHEC *lacZ* yielded colonies that are white on agar containing the chromogenic lactose analog 5-bromo-4-chloro-3-indolyl-β-D-galactopyranoside (X-gal). Derivatives of pTOX3 were also used to replace nearly 20 additional loci in EHEC.

Shigella flexneri is an increasingly antibiotic-resistant cause of dysentery. In *S. flexneri*, most secreted virulence proteins (effectors) are encoded by a large, unstable virulence plasmid. Recombineering is useful in performing single gene deletions on the plasmid, but multiple gene deletions leave identical scar sequences that can enable undesired recombination within the plasmid. pTOX3 was used to delete the virulence plasmid *ipgH* locus (Fig 3C) as well as chromosomal loci.

Finally, pTOX was efficacious in *Enterobacter cloacae,* an opportunistic hospital-associated pathogen associated with urinary tract and bloodstream infections. *E. cloacae,* like *S. marcescens,* possesses an inducible chromosomal beta-lactamase, AmpC, which hydrolyzes most beta-lactam antibiotics. A pTOX3 derivative was used to delete *E. cloacae ampC*. Colonies harboring the *ampC* deletion exhibited no detectable beta-lactamase activity, whereas colonies that reverted to wild-type *(ampC*$^{+}$*)* did (Figure 3D). Collectively, these observations suggest that pTOX may be widely useful in Gram-negative bacteria, particularly for those where other methods are difficult or unavailable.

Chromoproteins facilitate visual detection of pTOX transconjugants

Conjugation efficiency can vary between species and strains. For organisms like *S. marcescens,* in which conjugation can be inefficient, we incorporated an additional module coding for the AmilCP protein into the pTOX vectors (Fig 4A). AmilCP is a non-fluorescent blue chromoprotein derived from the *Acropora millepora* coral; we sought to use its blue coloration as an additional method to discriminate wild-type colonies from transconjugants. To this aim, multiple combinations of promoters and ribosomal binding sites were tested to identify those which provided coloration sufficient for discrimination without special equipment.

The series of *amilCP* modules were first tested in *E. coli* donors, where we found that the tac promoter (21) or the apFAB46 promoter (22) offered the deepest blue coloration (Fig 4B, Fig S3A). This level of *amilCP* expression did not incur a detectable fitness cost (Fig S3B); however, several strategies to increase colony coloration further (e.g increasing *amilCP* copy number) led to toxicity and were not pursued. pTOX vectors containing *amilCP* driven by the tac promoter and a pTOX vector expressing the magenta *tsPurple* chromoprotein driven by apFAB46 were created (Fig 4C) (23). Both AmilCP and TsPurple were visible in re-streaked merodiploid colonies after 24-48 hours of incubation (Fig 4D), though coloration was not as saturated as when expressed from the pTOX plasmids (which have medium-copy origins). Therefore, the pTOX chromoprotein modules may prove useful for monitoring the success of single- and double-crossover, particularly in organisms with inefficient conjugation.

Application of the pTOX vectors to study inducible antibiotic resistance

To further interrogate the utility of the pTOX suite, we used these vectors to characterize the role of the *S. marcescens* peptidoglycan (PG) amidohydrolases in inducible beta-lactam resistance mediated by the AmpC beta-lactamase. The PG component of the bacterial cell wall consists of a repeated disaccharide polymer linked through peptide cross-links. The peptidoglycan amidohydrolases facilitate remodeling of the cell wall by catalyzing hydrolysis of the amide bond linking the polysaccharide to the peptide component, generating muropeptide breakdown products that can subsequently be recycled in the cytoplasm (24). When the classical cytoplasmic PG amidohydrolase, *ampD,* becomes saturated with substrate in the setting of catastrophic remodeling precipitated by beta-lactam antibiotics such as penicillins and cephalosporins, the accumulation of muropeptides leads to *ampC* derepression. The associated beta-lactam resistance enables subsequent restoration of PG homeostasis (25).

In *E. cloacae* and *Citrobacter freundii,* expression of *ampC* at basal levels is sufficient for clinical resistance to penicillins and early-generation cephalosporins. After exposure to beta-lactams and the resulting accumulation of muropeptide breakdown products, transcriptional upregulation can lead to transient intermediate resistance to late-generation cephalosporins such as ceftriaxone. Under conditions where there is selection for high-level cephalosporin resistance (i.e. in individual patients who are subjected to prolonged cephalosporin treatment), mutation of the *ampD* amidohydrolase can occur. This leads to a constitutive increase in cytoplasmic muropeptide that is sufficient for high level derepression of *ampC* and resistance to ceftriaxone (26, 27). However, it is unclear whether the insights gained from studies of *E. cloacae* and *C. freundii* can be generalized to all AmpC-producing organisms, because the pathway to full derepression may be more complicated in organisms with multiple orthologous amidohydrolases. For example, in *Pseudomonas aeruginosa*, full derepression of *ampC* requires inactivation of additional *ampD* orthologues (28), while in *Yersinia enterocolitica*, deletion of all three *ampD* orthologues does not result in obvious clinical resistance (29).

Systematic investigation of the contribution of *S. marcescens* PG amidohydrolases to *ampC* derepression and resulting beta-lactam resistance has not been performed. We found that *S. marcescens* encodes 3 PG amidohydrolases, which, by sequence homology (30) we denote *ampD* (WP_033641266.1), *amiD* (WP_016928349.1), and *amiD2* (WP_048796451.1) (Fig 5A, Fig S4). Creation of pTOX derivatives targeting each of the *S. marcescens* PG amidohydrolases allowed the rapid generation of all combinations of single, double, and triple mutants (Fig. S5). We found that, of the single mutants, only Δ*amiD2* had a significant increase in basal AmpC activity (Fig. 5B); however, this corresponded to only a 2-fold increase in cephalosporin MICs (Table 2). In contrast, the Δ*ampD*Δ*amiD2* double mutant had a more than 50-fold increase in AmpC activity, which resulted in an 8-fold increase in the ceftriaxone and a 4-fold increase in cefepime MICs. The triple mutant exhibited no further increase in AmpC activity or in MICs. The Clinical and Laboratory

231 Standards Institute (CLSI) has recently updated their guidelines on MIC breakpoints above which
232 there is a potential for clinical resistance. Under the new breakpoints, the Δ*ampD*Δ*amiD2* double
233 mutant and triple mutant, with MICs of 2, would be considered to have “intermediate” resistance to
234 ceftriaxone, but to still be fully sensitive to ceftazidime and cefepime. In comparison, inactivation of
235 the single *E. cloacae ampD* was reported to result in a ceftriaxone MIC of 32 (from a baseline of
236 0.5) (26).
237
238 **Discussion**
239 Our findings suggest that the pTOX suite of allele exchange vectors described here should
240 facilitate the genetic engineering of diverse Proteobacteria. Each of the pTOX vectors includes a
241 rhamnose inducible toxin that may circumvent escape from counter selection, which can limit *sacB*-
242 based allele exchange vectors. These toxins have been used to facilitate recombineering (11), and
243 inducible toxins for allelic exchange promise to be a broadly generalizable approach, as systems
244 have recently also been described for Vibrio and Aeromonas species (31) as well as for the
245 archaeon *Pyrococcus yayanosii* (32).
246
247 The pTOX vectors contain an expanded multiple cloning site, multiple antibiotic resistance
248 cassettes, and chromoprotein modules that facilitate monitoring of crossover events. The utility of
249 the pTOX vectors and all 3 of the different toxins they encode was demonstrated through creation
250 of multiple deletions in 4 different pathogens, including *S. flexneri*, an organism in which allele
251 exchange has been difficult. All of these vectors have been deposited at Addgene to facilitate their
252 distribution. Besides their utility for engineering Gram-negative organisms in research labs, these
253 vectors may also be useful in the context of undergraduate education.
254
255 *S. marcescens,* along with *E. cloacae*, *C. freundii, Klebsiella aerogenes* and *Morganella morganii*,
256 are members of a group of pathogenic *Enterobacteriaceae* with the potential for high level,

257 inducible expression of AmpC, which in some cases has been linked to resistance to almost all
258 penicillins and cephalosporins (33). Original reports of cephalosporin failure in *E. cloacae* (34)
259 engendered the practice of using ultra-broad spectrum antibiotics (such as cefepime or
260 carbapenems, which are resistant to AmpC hydrolysis) in the treatment of serious infections by
261 pathogens with the potential for AmpC overexpression. However, this approach has untoward
262 consequences, including increasing infections with carbapenem-resistant Enterobacteriaceae (35).
263
264 It is not clear if routine use of ultra-broad spectrum antibiotics is warranted for all organisms with
265 inducible AmpC expression. A recent review (36) emphasized that besides *E. cloacae,* the data on
266 cephalosporin failure for pathogens with inducible AmpC is sparse. What data do exist emphasize
267 that true on-treatment emergence of beta-lactam resistance is probably rare, at least in *S.*
268 *marcescens* and in *Morganella morganii (37)*. *In vitro* experiments also hint at important
269 heterogeneity among these pathogens; in this setting, the development of spontaneous
270 cephalosporin resistance has been reported to be nearly 100-fold lower in *S. marcescens*
271 compared to *E. cloacae* and *C. freundii*, and 10-fold lower still in *M. morganii* (38).
272
273 Our observations suggest that ultra-broad-spectrum antibiotics may be not be necessary for
274 treatment of *S. marcescens* infections. We used the pTOX vectors to investigate the role of *S.*
275 *marcescens'* 3 peptidoglycan amidohydrolases on inducible beta-lactam antibiotic resistance. We
276 found that deletion of a single amidohydrolase locus had a minimal effect on cephalosporin MICs,
277 and that even the absence of all 3 amidohydrolase loci did not consistently render *S. marcescens*
278 resistant to this class of antibiotics, although the triple mutant and the *ΔampDΔamiD2* double
279 mutant did exhibit intermediate resistance to ceftriaxone. Thus, the effects of amidohydrolase
280 deletion in *S. marcescens* differ from those in *C. freundii* and *E. cloacae,* in which resistance arises
281 following the loss of a single amidohydrolase. Importantly, though current CLSI breakpoints would
282 classify the *ΔampDΔamiD2* double mutant as having "Intermediate" resistance to ceftriaxone, there

283 is no evidence of increased clinical failure in this range (39). This is important since ceftriaxone is
284 less expensive, has more convenient dosing intervals, and is a narrower spectrum agent compared
285 to cefepime or carbapenems. Further work with additional *S. marcescens* isolates to clarify the
286 generalizability of our findings is warranted.
287
288 **Materials and Methods**
289
290 pTOX construction
291 The DNA components for the pTOX series were obtained from pDS132 (15), the pSLC
292 recombineering series (11) which was a gift from Swaine Chen (Addgene plasmid # 73194),
293 pON.mCherry (21) which was a gift from Howard Shuman (Addgene plasmid # 84821), strain
294 TP997 (40) which was a gift from Anthony Poteete (Addgene plasmid # 13055), and direct gene
295 synthesis (from Integrated DNA Technologies) and were assembled using Gibson or HiFi
296 Assembly (New England BioLabs) unless otherwise stated. All restriction enzymes were obtained
297 from New England Biolabs and all PCR was performed with primers from Integrated DNA
298 Technologies and Q5 polymerase (New England Biolabs). All cloning steps were performed in π-
299 carrying hosts (either DH5αpir (41) for propagation or MFD-π (42) for conjugation) under catabolite
300 repression in LB containing the appropriate antibiotic and 2% glucose (w/v).
301
302 pSLC toxin vectors were first linearized with primers prJL1 and prJL2 and joined with the fragment
303 obtained from pDS132 with primers prJL3 and prJL4 (see Supplemental Table 1 for all primers
304 used in this study). The mobRP4 from pDS132 was subsequently amplified with primers prJL5 and
305 prJL6 and assembled with the prior vectors cut with NheI. The chloramphenicol resistance cassette
306 from pON.mCherry was then amplified with primers prJL7 and prJL8 and inserted into the prior
307 vectors digested with ClaI and BglII. The π-dependent origin from pDS132 was next isolated by
308 SmaI-digestion and inserted into the prior vectors linearized with prJL9 and prJL10. A codon-

optimized *rhaS* (with the original primary protein sequence obtained from WP_000217135.1) and promoter (see Supplemental Text 1 for the sequence of all directly synthesized DNA fragments used in this study) was obtained by direct synthesis and assembled into the prior vectors linearized with prJL11 and prJL12. The expanded polylinker (19) with the forward transcriptional terminator BBa_B1002 (IGEM) was obtained by direct synthesis (Sequence 2) and inserted into the prior vectors linearized with primers prJL13 and prJL14. The artificial ribosome binding site was generated using the online calculator derived after (17), synthesized as above (Sequence 3) and assembled into the prior vectors linearized with prJL15 and prJL16 to generate pTOX1 (containing *yhaV*), pTOX2 (containing *mqsR*) and pTOX3 (containing *tse2)*. See Supplemental Table 2 for all plasmids used in this work. For insertion of *amilCP* or *tsPurple*, the above vectors were cut with SbfI and Sequence 4 and Sequence 5 inserted. For replacement of the chloramphenicol resistance cassette with one encoding gentamicin resistance, the appropriate vector was linearized with prJL17 and prJL18 and assembled with the cassette amplified from strain TP997 (using prJL19 and prJL20). See Supplemental Table 3 for all strains used in this work. Q5 GC enhancer (New England Biolabs) was used for amplification of mobRP4 and *tse2*.

Insertion of homology targeting regions

pTOX vectors were cut with SmaI and the relevant homologous regions were assembled after being amplified with prJL21, prJL22, prJL23, and prJL24 (for *S. marcescens hexS);* prAW1, prAW2, prAW3, and prAW4 (for EHEC *lacZ)*; prCJK1, prCJK2, prCJK3, and prCJK4 (for *S. flexneri ipgH);* prJL25, prJL26, prJL27, and prJL28 (for *E. cloacae ampC)*; prJL29, prJL30, prJL31, and prJL32 (for *S. marcescens ampD*); prJL33, prJL34, prJL35, and prJL36 (for *S. marcescens amiD*); and prJL37, prJL38, prJL39, and prJL40 (for *S. marcescens amiD2*). Note that some of the overlap regions in the above primers correspond to a version of pTOX with the original pDS132 polylinker.

Allelic exchange with pTOX

335 On day 1, the appropriate upstream and downstream sequences from the targeted pathogen are
336 amplified from gDNA in separate PCR reactions. After column purification of the resulting PCR
337 product (Denville), the products are assembled with pTOX previously gel-purified after restriction
338 digestion of the polylinker and electroporated into an *E. coli* strain that could serve as donor in
339 conjugation. Throughout this work, we routinely used the diaminopimelic acid (DAP) auxotroph
340 MFD-π (42) as the pTOX donor strain. Unless specified, all subsequent steps are performed in the
341 presence of 2% glucose to avoid premature toxin induction. On day 2, colony PCR was performed
342 on single MFD-π transformant colonies to confirm the appropriate insert size. On day 3,
343 conjugation was performed between the MFD-π bearing pTOX and the pathogen of interest.
344 Optimizing the conjugation is crucial. For example, we found that conjugation was efficient at 4-8
345 hours at 37°C with a 3:1 (v/v) ratio of MFD-π:pathogen for EHEC, *E. cloacae*, and *S. flexneri,* but
346 *S. marcescens* had markedly better efficiency when conjugated overnight at 30°C using 50-fold
347 excess volume of an early logarithmic phase growth culture of MFD-π. Exconjugants were isolated
348 on appropriate antibiotics. On day 4, a single exconjugant colony is resuspended in 2 mL of LB
349 containing glucose (but no selective antibiotic). This culture is incubated at 37°C with agitation until
350 OD_{600} 0.2, then washed twice with M9 salts (Sigma) with 2% rhamnose (w/v) before plating on the
351 M9-rhamnose agar described below. A short preliminary outgrowth in broth without selection
352 minimizes the possibility of the culture becoming dominated with a single double-crossover
353 rhamnose-resistant clone. On day 5, the desired mutants can be identified with colony PCR on the
354 resulting double-crossover colonies. The selection is stringent and in this manner, individual
355 colonies can frequently be isolated from a plate inoculated with the undiluted washed culture from
356 above, but 10^{-1} and 10^{-2} dilutions should also be plated.
357
358 For the experiments described in Table 1, primers prJL51 and prJL52 were used; their amplicon
359 consisted of a small intergenic region that was largely replaced when the expanded polylinker was
360 inserted.

361

362 *amilCP* coloration optimization

363 pTOX derivatives with different promoters and ribosome binding sites to drive *amilCP* were created
364 by assembling SbfI-cut pTOX1 with *amilCP* (Sequence 4) amplified with prJL59 and either prJL41
365 (for J23119-B0030), prJL42 (for J23119-B0034), prJL43 (for CP25-B0030), or prJL44 (for
366 apFAB46-B0030). The J23119 promoter and B0030 and B0034 ribosome binding sites sequences
367 were obtained from IGEM. The insulated proD promoter (43) was amplified from pSB3C5-proD-
368 B0032-E0051 (which was a gift from Joseph Davis and Robert Sauer; Addgene plasmid #107241)
369 with prJL47 and prJL48, fused by SOE PCR with the *amilCP* coding sequence obtained from PGR-
370 Blue (44) (which was a gift from Nathan Reyna; Addgene plasmid #68374) using prJL49 and
371 prJL50, and after XbaI-digestion of this product, it was ligated with XbaI-cut pTOX1. The J23119-
372 synthetic ribosome binding site (17) was amplified from Sequence 6 with prJL45 and prJL46 and
373 assembled in SbfI-cut vector and *amilCP* amplified with prJL49 and prJL50 as for proD above.

374

375 *E. coli* DH5αpir were transformed with the appropriate *amilCP*-containing plasmid. Single colonies
376 were grown in overnight cultures, diluted 1:100, and then back-diluted once in logarithmic phase
377 growth so to enable spot-streaking onto solid agar at the identical optical density. Digital images
378 were taken at 24h and 48h and saturation obtained by splitting the resulting image into an “HSB
379 Stack” in ImageJ. The peak saturation was subsequently obtained using the “Measure” function,
380 then normalized by subtracting the peak saturation of the resulting spots from spots of *E. coli*
381 DH5αpir carrying pTOX1 without *amilCP.* The resulting values represent the mean ± SEM of this
382 procedure done on 3 different days.

383

384 Beta-lactamase assay

385 Overnight cultures of indicated strains were back-diluted 1:100 (v/v) into fresh media and grown for
386 an additional 2 hours. Bacteria were then pelleted, washed twice in phosphate-buffered saline, and

387 then flash-frozen in liquid nitrogen. On the day of the assay, pellets were thawed at 37°C and then
388 subjected to a single round of sonication on ice (Sonic Dismembranator 60, Fisher Scientific,
389 setting 8, 5 seconds). Lysates were clarified by centrifugation at 20,000 rcf for 60 minutes at 4°C.
390 Total protein was quantitated by fluorometry using the Qbit Protein Assay Kit (Thermo Fisher).
391 Beta-lactamase activity was determined by the addition of 80 ng nitrocefin to either 250 ng or 1000
392 ng of total protein; to facilitate accurate quantitation, 250 ng was used for all cefoxitin-induced *S.*
393 *marcescens* samples and also for the Δ*ampD*Δ*amiD2* double mutant and the triple mutant.
394 Immediately after addition of nitrocefin with a multi-channel pipettor, absorbance was read
395 kinetically at 495 nm every 5 minutes in a Synergy HT plate reader (BioTek). For Figure 5, the
396 slope of the absorbance was normalized to wild-type *S. marcescens* and the amount of total
397 protein added.
398
399 Minimum inhibitory concentration (MIC) determination
400 Minimum inhibitory concentrations were determined for the indicated *S. marcescens* isolates and
401 performed by broth microdilution according to CLSI guidelines and after Weigand *et al (45)*. Briefly,
402 overnight cultures were back-diluted in cation-adjusted Mueller-Hinton broth, allowed to grow for 2
403 hours, and adjusted to a final inoculum of 5 x 10^5 colony-forming units per mL before applying to
404 wells with the appropriate antibiotic concentration. Results were read after 20 hours of incubation
405 at 37°C. The results in Table 2 represent the mode of 3 independent experiments.
406
407 Materials and strains
408 Unless otherwise specified, all materials were purchased from Sigma. When appropriate, media
409 was supplemented with streptomycin 200 µg/mL, gentamicin 5 µg/mL, and chloramphenicol 20
410 µg/mL for all *E. coli*, *E. cloacae,* and *S. flexneri. S. marcescens* exconjugants were isolated at 100
411 µg/mL chloramphenicol. Diaminopimelic acid (DAP) was used at a final concentration of 0.3 mM, 5-
412 bromo-4-chloro-3-indolyl-β-D-galactopyranoside (X-gal) at 60 µg/mL, glucose at 2% (w/v) in all

propagation steps with pTOX vectors. When washing the out-grown single-crossovers, rhamnose was used at 2% (w/v) in M9 salts. The resulting washed bacteria were plated on M9 agar supplemented with 0.2% casamino acids (w/v), 0.5 mM $MgSO_4$, 0.1 mM $CaCl_2$, 25 uM iron chloride in 50 uM citric acid, the appropriate antibiotic, and rhamnose. Rhamnose at a final concentration of 0.2%-2% facilitated good toxin induction in the organisms we tested; there was no obvious correlation with the concentration of rhamnose used, but it may be prudent to optimize this in new organisms. The *S. marcescens* ATCC 13880 isolate used throughout this work is a spontaneous mutant selected on streptomycin. *E. cloacae* was obtained from ATCC (isolate 13047). EHEC was isolate EDL933. *S. flexneri* was strain 2457T.

Miscellaneous analysis

All figures and statistical analyses were prepared in Prism 8 (Graphpad). The growth curves in Supplemental Figure 3 were generated using Bioscreen C (Growth Curves USA). The plasmid maps were generated with AngularPlasmid and ApE (for the polylinker inset in Figure 1).

Acknowledgments

JEL has been supported by T32 AI-007061 and by the Harvard Catalyst Medical Research Investigator Training fellowship; ARW by T32AI132120; MKW by R01 AI-042347 and HHMI. We thank the other members of our group for many productive conversations informing the design of pTOX and for comments on the manuscript.

References

1. Thomason LC, Sawitzke JA, Li X, Costantino N, Court DL. 2014. Recombineering: genetic engineering in bacteria using homologous recombination. Curr Protoc Mol Biol 106:1.16.1–39.

2. Jiang W, Bikard D, Cox D, Zhang F, Marraffini LA. 2013. RNA-guided editing of bacterial

438 genomes using CRISPR-Cas systems. Nat Biotechnol 31:233–239.

439 3. Pyne ME, Moo-Young M, Chung DA, Chou CP. 2015. Coupling the CRISPR/Cas9 System
440 with Lambda Red Recombineering Enables Simplified Chromosomal Gene Replacement in
441 Escherichia coli. Appl Environ Microbiol 81:5103–5114.

442 4. Reisch CR, Prather KLJ. 2015. The no-SCAR (Scarless Cas9 Assisted Recombineering)
443 system for genome editing in Escherichia coli. Sci Rep 5:15096.

444 5. Link AJ, Phillips D, Church GM. 1997. Methods for generating precise deletions and insertions
445 in the genome of wild-type Escherichia coli: application to open reading frame
446 characterization. J Bacteriol 179:6228–6237.

447 6. Miller VL, Mekalanos JJ. 1988. A novel suicide vector and its use in construction of insertion
448 mutations: osmoregulation of outer membrane proteins and virulence determinants in Vibrio
449 cholerae requires toxR. J Bacteriol 170:2575–2583.

450 7. Reyrat JM, Pelicic V, Gicquel B, Rappuoli R. 1998. Counterselectable markers: untapped tools
451 for bacterial genetics and pathogenesis. Infect Immun 66:4011–4017.

452 8. Maloy SR, Nunn WD. 1981. Selection for loss of tetracycline resistance by Escherichia coli. J
453 Bacteriol 145:1110–1111.

454 9. Hmelo LR, Borlee BR, Almblad H, Love ME, Randall TE, Tseng BS, Lin C, Irie Y, Storek KM,
455 Yang JJ, Siehnel RJ, Howell PL, Singh PK, Tolker-Nielsen T, Parsek MR, Schweizer HP,
456 Harrison JJ. 2015. Precision-engineering the Pseudomonas aeruginosa genome with two-step
457 allelic exchange. Nat Protoc 10:1820–1841.

458 10. Li X-T, Thomason LC, Sawitzke JA, Costantino N, Court DL. 2013. Positive and negative
459 selection using the tetA-sacB cassette: recombineering and P1 transduction in Escherichia
460 coli. Nucleic Acids Res 41:e204.

461 11. Khetrapal V, Mehershahi K, Rafee S, Chen S, Lim CL, Chen SL. 2015. A set of powerful
462 negative selection systems for unmodified Enterobacteriaceae. Nucleic Acids Res 43:e83.

463 12. Mahlen SD. 2011. Serratia infections: from military experiments to current practice. Clin
464 Microbiol Rev 24:755–791.

465 13. O'Rear J, Alberti L, Harshey RM. 1992. Mutations that impair swarming motility in Serratia
466 marcescens 274 include but are not limited to those affecting chemotaxis or flagellar function.
467 J Bacteriol 174:6125–6137.

468 14. Reid JD, Stoufer SD, Ogrydziak DM. 1982. Efficient transformation of Serratia marcescens
469 with pBR322 plasmid DNA. Gene 17:107–112.

470 15. Philippe N, Alcaraz J-P, Coursange E, Geiselmann J, Schneider D. 2004. Improvement of
471 pCVD442, a suicide plasmid for gene allele exchange in bacteria. Plasmid 51:246–255.

472 16. Kelly CL, Liu Z, Yoshihara A, Jenkinson SF, Wormald MR, Otero J, Estévez A, Kato A,
473 Marqvorsen MHS, Fleet GWJ, Estévez RJ, Izumori K, Heap JT. 2016. Synthetic Chemical
474 Inducers and Genetic Decoupling Enable Orthogonal Control of the rhaBAD Promoter. ACS
475 Synth Biol 5:1136–1145.

476 17. Espah Borujeni A, Channarasappa AS, Salis HM. 2014. Translation rate is controlled by
477 coupled trade-offs between site accessibility, selective RNA unfolding and sliding at upstream
478 standby sites. Nucleic Acids Res 42:2646–2659.

479 18. Giacalone MJ, Gentile AM, Lovitt BT, Berkley NL, Gunderson CW, Surber MW. 2006. Toxic
480 protein expression in Escherichia coli using a rhamnose-based tightly regulated and tunable
481 promoter system. Biotechniques 40:355–364.

482 19. Latynski US, Valentovich LN. 2014. DNA tuner: a computer program for the construction of
483 polylinker sequences of molecular vectors. Proceedings of the Belarusian State University

Series of Physiological, Biochemical and Molecular Biology Sciences 9:148–153.

20. Tanikawa T, Nakagawa Y, Matsuyama T. 2006. Transcriptional downregulator hexS controlling prodigiosin and serrawettin W1 biosynthesis in Serratia marcescens. Microbiol Immunol 50:587–596.

21. Gebhardt MJ, Jacobson RK, Shuman HA. 2017. Seeing red; the development of pON.mCherry, a broad-host range constitutive expression plasmid for Gram-negative bacteria. PLoS One 12:e0173116.

22. Kosuri S, Goodman DB, Cambray G, Mutalik VK, Gao Y, Arkin AP, Endy D, Church GM. 2013. Composability of regulatory sequences controlling transcription and translation in Escherichia coli. Proc Natl Acad Sci U S A 110:14024–14029.

23. Liljeruhm J, Funk SK, Tietscher S, Edlund AD, Jamal S, Wistrand-Yuen P, Dyrhage K, Gynnå A, Ivermark K, Lövgren J, Törnblom V, Virtanen A, Lundin ER, Wistrand-Yuen E, Forster AC. 2018. Engineering a palette of eukaryotic chromoproteins for bacterial synthetic biology. J Biol Eng 12:8.

24. Rivera I, Molina R, Lee M, Mobashery S, Hermoso JA. 2016. Orthologous and Paralogous AmpD Peptidoglycan Amidases from Gram-Negative Bacteria. Microb Drug Resist 22:470–476.

25. Johnson JW, Fisher JF, Mobashery S. 2013. Bacterial cell-wall recycling. Ann N Y Acad Sci 1277:54–75.

26. Guérin F, Isnard C, Cattoir V, Giard JC. 2015. Complex Regulation Pathways of AmpC-Mediated β-Lactam Resistance in Enterobacter cloacae Complex. Antimicrob Agents Chemother 59:7753–7761.

27. Kopp U, Wiedemann B, Lindquist S, Normark S. 1993. Sequences of wild-type and mutant

507 ampD genes of Citrobacter freundii and Enterobacter cloacae. Antimicrob Agents Chemother
508 37:224–228.

509 28. Moya B, Juan C, Albertí S, Pérez JL, Oliver A. 2008. Benefit of having multiple ampD genes
510 for acquiring beta-lactam resistance without losing fitness and virulence in Pseudomonas
511 aeruginosa. Antimicrob Agents Chemother 52:3694–3700.

512 29. Liu C, Wang X, Chen Y, Hao H, Li X, Liang J, Duan R, Li C, Zhang J, Shao S, Jing H. 2016.
513 Three Yersinia enterocolitica AmpD Homologs Participate in the Multi-Step Regulation of
514 Chromosomal Cephalosporinase, AmpC. Front Microbiol 7:1282.

515 30. Kumar S, Stecher G, Li M, Knyaz C, Tamura K. 2018. MEGA X: Molecular Evolutionary
516 Genetics Analysis across Computing Platforms. Mol Biol Evol 35:1547–1549.

517 31. Wiles TJ, Wall ES, Schlomann BH, Hay EA, Parthasarathy R, Guillemin K. 2018. Modernized
518 Tools for Streamlined Genetic Manipulation and Comparative Study of Wild and Diverse
519 Proteobacterial Lineages. MBio 9.

520 32. Song Q, Li Z, Chen R, Ma X, Xiao X, Xu J. 2018. Induction of a toxin-antitoxin gene cassette
521 under high hydrostatic pressure enables markerless gene disruption in the hyperthermophilic
522 archaeon Pyrococcus yayanosii. Appl Environ Microbiol.

523 33. Jacoby GA. 2009. AmpC beta-lactamases. Clin Microbiol Rev 22:161–182.

524 34. Chow JW, Fine MJ, Shlaes DM, Quinn JP, Hooper DC, Johnson MP, Ramphal R, Wagener
525 MM, Miyashiro DK, Yu VL. 1991. Enterobacter bacteremia: clinical features and emergence of
526 antibiotic resistance during therapy. Ann Intern Med 115:585–590.

527 35. Chiotos K, Tamma PD, Flett KB, Naumann M, Karandikar MV, Bilker WB, Zaoutis T, Han JH.
528 2017. Multicenter Study of the Risk Factors for Colonization or Infection with Carbapenem-
529 Resistant Enterobacteriaceae in Children. Antimicrob Agents Chemother 61.

530 36. Tamma PD, Doi Y, Bonomo RA, Johnson JK, Simner PJ, Antibacterial Resistance Leadership
531 Group. 2019. A Primer on AmpC Beta-Lactamases: Necessary Knowledge for an Increasingly
532 Multidrug-Resistant World. Clin Infect Dis.

533 37. Choi S-H, Lee JE, Park SJ, Choi S-H, Lee S-O, Jeong J-Y, Kim M-N, Woo JH, Kim YS. 2008.
534 Emergence of antibiotic resistance during therapy for infections caused by Enterobacteriaceae
535 producing AmpC beta-lactamase: implications for antibiotic use. Antimicrob Agents Chemother
536 52:995–1000.

537 38. Kohlmann R, Bähr T, Gatermann SG. 2018. Species-specific mutation rates for ampC
538 derepression in Enterobacterales with chromosomally encoded inducible AmpC β-lactamase.
539 J Antimicrob Chemother.

540 39. Tamma PD, Pierce VM, Cosgrove SE, Lautenbach E, Harris A, Rayapati D, Han JH. 2018.
541 Can the Ceftriaxone Breakpoints Be Increased Without Compromising Patient Outcomes?
542 Open Forum Infect Dis 5:ofy139.

543 40. Poteete AR, Rosadini C, St. Pierre C. 2006. Gentamicin and other cassettes for chromosomal
544 gene replacement in Escherichia coli. Biotechniques 41:261–264.

545 41. Platt R, Drescher C, Park SK, Phillips GJ. 2000. Genetic system for reversible integration of
546 DNA constructs and lacZ gene fusions into the Escherichia coli chromosome. Plasmid 43:12–
547 23.

548 42. Ferrieres L, Hemery G, Nham T, Guerout A-M, Mazel D, Beloin C, Ghigo J-M. 2010. Silent
549 Mischief: Bacteriophage Mu Insertions Contaminate Products of Escherichia coli Random
550 Mutagenesis Performed Using Suicidal Transposon Delivery Plasmids Mobilized by Broad-
551 Host-Range RP4 Conjugative Machinery. J Bacteriol 192:6418–6427.

552 43. Davis JH, Rubin AJ, Sauer RT. 2011. Design, construction and characterization of a set of

553 insulated bacterial promoters. Nucleic Acids Res 39:1131–1141.

554 44. Bradshaw JC, Gongola AB, Reyna NS. 2016. Rapid Verification of Terminators Using the
555 pGR-Blue Plasmid and Golden Gate Assembly. J Vis Exp.

556 45. Wiegand I, Hilpert K, Hancock REW. 2008. Agar and broth dilution methods to determine the
557 minimal inhibitory concentration (MIC) of antimicrobial substances. Nat Protoc 3:163–175.

558 **Tables**

559

560 **TABLE 1** Absence of integrated pTOX in putative double-crossover colonies[a]

	YhaV toxin	MqsR toxin	Tse2 toxin
CAM^R	0/69	0/69	0/69
PCR$^+$	0/69	0/69	0/69

561 [a] CAM = chloramphenicol resistance was determined using the parental single-
562 crossover colony as a positive control. An intergenic region of pTOX was used for
563 colony PCR to avoid false negatives during selection for inactivated open reading
564 frames.

565

566

567 **TABLE 2** Minimal inhibitory concentrations for amidohydrolase mutants[b]

	MIC (μg/mL)			
Strain	**FOX**	**CTX**	**CAZ**	**FEP**

S. marcescens ATCC 13880	16	0.13	0.25	0.06
SM Δ*ampD*	16	0.13	0.25	0.03
SM Δ*amiD*	16	0.13	0.25	0.13
SM Δ*amiD2*	16	0.25	0.50	0.13
SM Δ*ampD*Δ*amiD*	16	0.50	0.25	0.13
SM Δ*ampD*Δ*amiD2*	16	2.00	0.50	0.25
SM Δ*amiD*Δ*amiD2*	16	0.13	0.25	0.06
SM Δ*ampD*Δ*amiD*Δ*amiD2*	16	2.00	0.50	0.25

[b] MICs for indicated strain were calculated using broth microdilution according to CLSI Guidelines. SM, *S. marcescens* ATCC strain 13880. FOX, cefoxitin; CTX, ceftriaxone; CAZ, ceftazidime; FEP, cefepime.

571 **Figure Legends**

572 **Fig 1** Allelic exchange with pTOX. A) Plasmid map of pTOX1. R6Kori, the R6K origin of replication;
573 mobRP4, mobilization region from RP4 conjugative plasmid; *rhaS*, the rhamnose transcriptional
574 activator; MCS, multiple cloning site; Cam-R, chloramphenicol resistance cassette; pRha,
575 rhamnose promoter. Vertical black bars of varying width represent terminators. Bottom, expanded
576 polylinker with restriction sites unique to pTOX1 (*yhaV*) shown. Red arrow, forward transcriptional
577 terminator. B) pTOX workflow. Step 1: the desired allele is inserted into the MCS using isothermal
578 assembly and transformed into donor *E. coli*. (yellow bacillus) Step 2: conjugation is performed
579 between the donor *E. coli* and the organism of interest (red coccobacillus). Step 3: pTOX
580 integrates into the appropriate chromosomal locus. Step 4: merodiploids are isolated and toxin
581 induced. Step 5: the desired clone is identified by colony PCR.
582
583 **Fig 2** Induction of specific bacterial toxins inhibit *S. marcescens* growth. *S. marcescens* wild-type
584 (Wt) or merodiploid (merodip) harboring the indicated pTOX-carrying toxin were diluted from
585 exponential phase growth in LB into either 2% (w/v) glucose (gluc) or rhamnose-containing (rham)
586 LB and incubated with agitation at 37^{O}C. Note that the Wt (gluc) curve is obscured by the Wt
587 (rham) curve in A and the error bars in C are smaller than the line for all but the merodiploid (gluc).
588 Means and SEM are depicted from at least 3 independently generated merodiploids.
589
590 **Fig 3** pTOX for genomic modification in multiple pathogens. A) *S. marcescens* colony coloration in
591 Wt (left) *and* Δ*hexS* (right) grown at 37^{O}C for 1 day. HexS inhibits expression of the red prodigiosin
592 characteristic of *S. marcescens.* B) *E. coli* O157:H7 colony coloration in Wt (left) and Δ*lacZ* (right)
593 grown on X-gal-containing media. Blue-green colony color indicates lactose fermentation. C) *S.*
594 *flexneri* colony PCR and results of 1% agarose gel electrophoresis demonstrating deletion of
595 *ipgH* from *S. flexneri* virulence plasmid. M, marker; Wt, wild-type; Δ, Δ*ipgH*. D) *E. cloacae* beta-
596 lactamase activity in total clarified sonicate from 3 Wt double-crossover colonies and from 3

597 Δ*ampC* colonies. Sonicates were incubated with nitrocefin, a chromogenic cephalosporin substrate
598 which absorbs at 495 nm when hydrolyzed.
599
600 **Fig 4** A chromoprotein module facilitates monitoring of conjugation. A) Plasmid map of pTOX4.
601 R6Kori, the R6K origin of replication; mobRP4, mobilization region from RP4 conjugative
602 plasmid; *rhaS*, the rhamnose transcriptional activator; *amilCP*, the blue amilCP chromoprotein;
603 MCS, multiple cloning site; Cam-R, chloramphenicol resistance cassette; pRha, rhamnose
604 promoter. Vertical black bars of varying width represent terminators. B) tac and apFAB46-B0030
605 allow optimal amilCP expression. Relative color saturation at 24h and at 48h of pTOX4-containing
606 colonies with various promoters and ribosome-binding sites (described in more detail in the
607 Methods). C) Depiction of donor *E. coli* containing (from bottom, clockwise) pTOX without
608 chromoprotein, with tac-*amilCP*, and with apFAB46-B0030-*tsPurple* after 24h at 37^{O}C. D) *E.*
609 *cloacae* pTOX merodiploids (from bottom, clockwise) without chromoprotein, with tac-*amilCP* ,
610 and with apFAB46-B0030-*tsPurple* after 24h at 37^{O}C and an additional 24 hours at 25^{O}C.
611
612 **Fig 5** *S. marcescens* peptidoglycan amidohydrolase deletions lead to differential derepression of
613 *ampC.* A) Phylogenetic analysis performed using the Maximum Likelihood method and JTT matrix-
614 based model in MEGA X (30)An unrooted tree is shown with the lowest log likelihood (-4913). B)
615 Clarified sonicates from indicated strains were incubated with equal amounts of nitrocefin, a
616 chromogenic cephalosporin beta-lactam, and absorbance measured in kinetic mode for 10
617 minutes. The slope of the line from the first 5 data points were used to calculate beta-lactamase
618 activity, which was then normalized to Wt. Measurements are shown either without pre-induction,
619 and those with induction with cefoxitin 4 μg/mL for 2 hours prior to harvesting. Data represent the
620 mean ± SEM of 4 independent experiments. Comparisons were made between all uninduced
621 mutants and Wt, and between each induced sample and its uninduced control. * = $p < 0.05$ after
622 performing Bonferroni correction. All induced samples are also significantly different from their

623 uninduced samples, except for Δ*ampD*Δ*amiD*, Δ*ampD*Δ*amiD2*, and the triple mutant. These

624 asterisks are not shown for clarity.

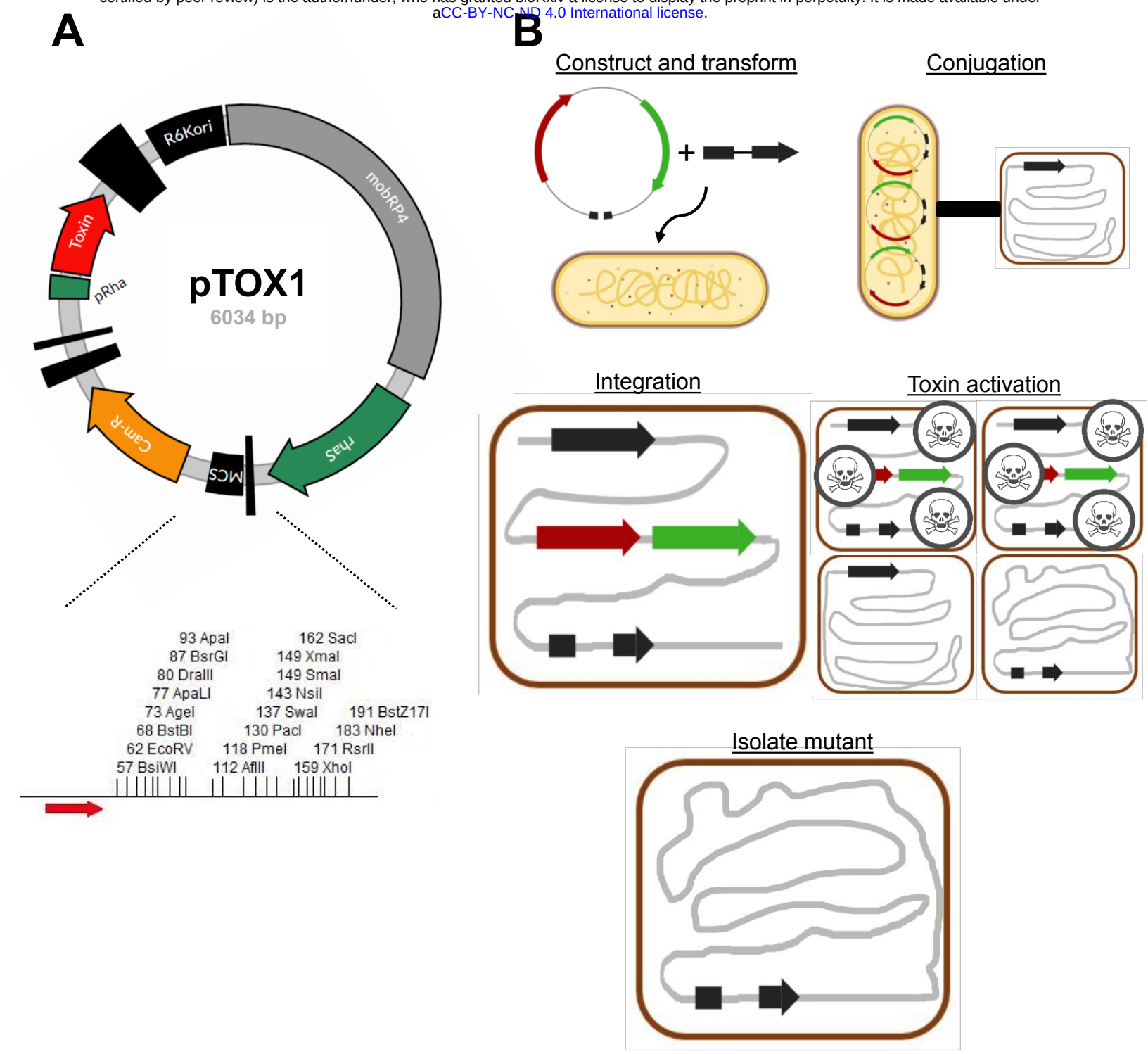

Fig 1 Allelic exchange with pTOX. A) Plasmid map of pTOX1. R6Kori, the R6K origin of replication; mobRP4, mobilization region from RP4 conjugative plasmid; *rhaS*, the rhamnose transcriptional activator; MCS, multiple cloning site; Cam-R, chloramphenicol resistance cassette; pRha, rhamnose promoter. Vertical black bars of varying width represent terminators. Bottom, expanded polylinker with restriction sites unique to pTOX1 (*yhaV*) shown. Red arrow, forward transcriptional terminator. B) pTOX workflow. Step 1: the desired allele is inserted into the MCS using isothermal assembly and transformed into donor *E. coli*. (yellow bacillus) Step 2: conjugation is performed between the donor *E. coli* and the organism of interest (red coccobacillus). Step 3: pTOX integrates into the appropriate chromosomal locus. Step 4: merodiploids are isolated and toxin induced. Step 5: the desired clone is identified by colony PCR.

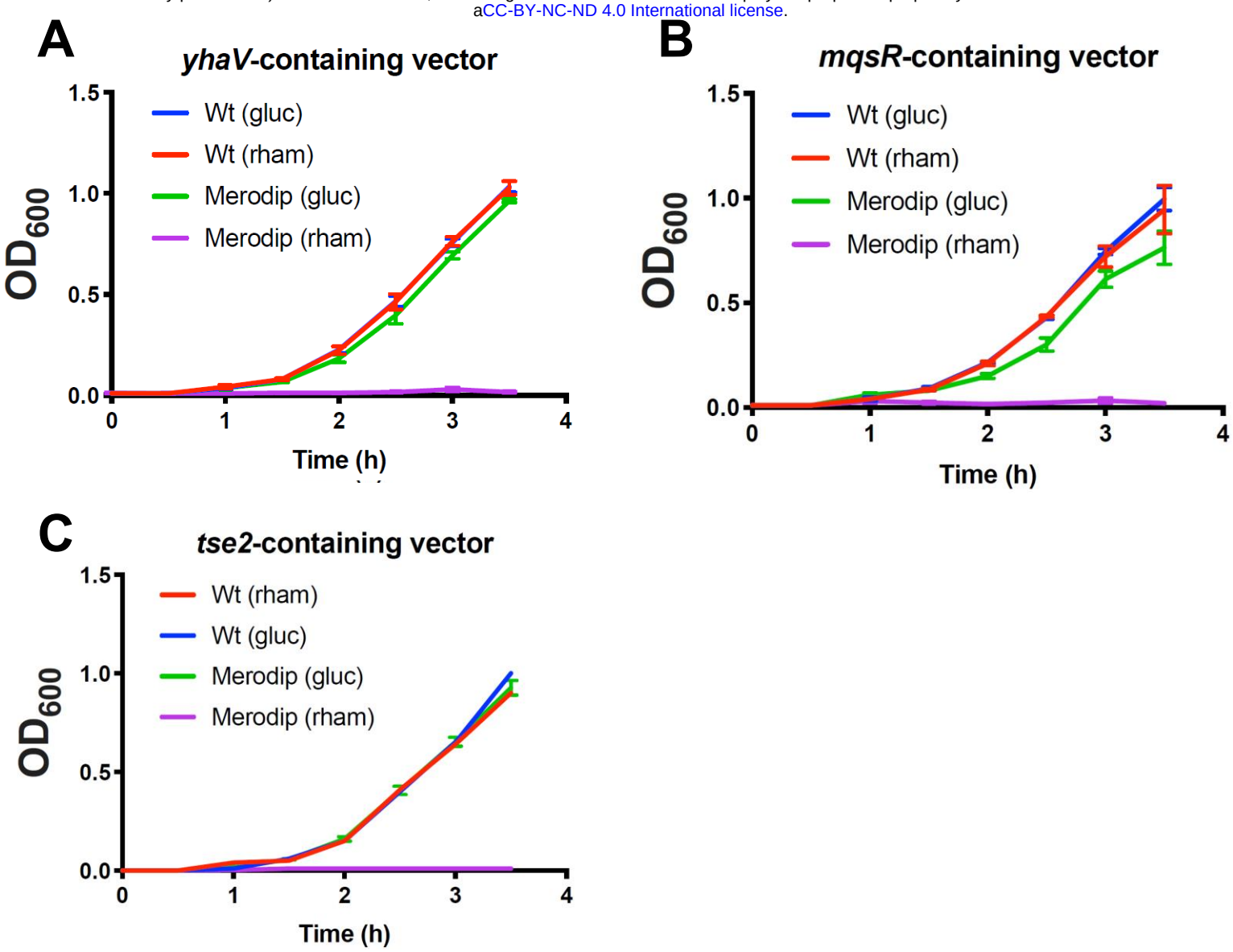

Fig 2 Induction of specific bacterial toxins inhibit *S. marcescens* growth. *S. marcescens* wild-type (Wt) or merodiploid (merodip) harboring the indicated pTOX-carrying toxin were diluted from exponential phase growth in LB into either 2% (w/v) glucose (gluc) or rhamnose-containing (rham) LB and incubated with agitation at 37^{O}C. Note that the Wt (gluc) curve is obscured by the Wt (rham) curve in A and the error bars in C are smaller than the line for all but the merodiploid (gluc). Means and SEM are depicted from at least 3 independently generated merodiploids.

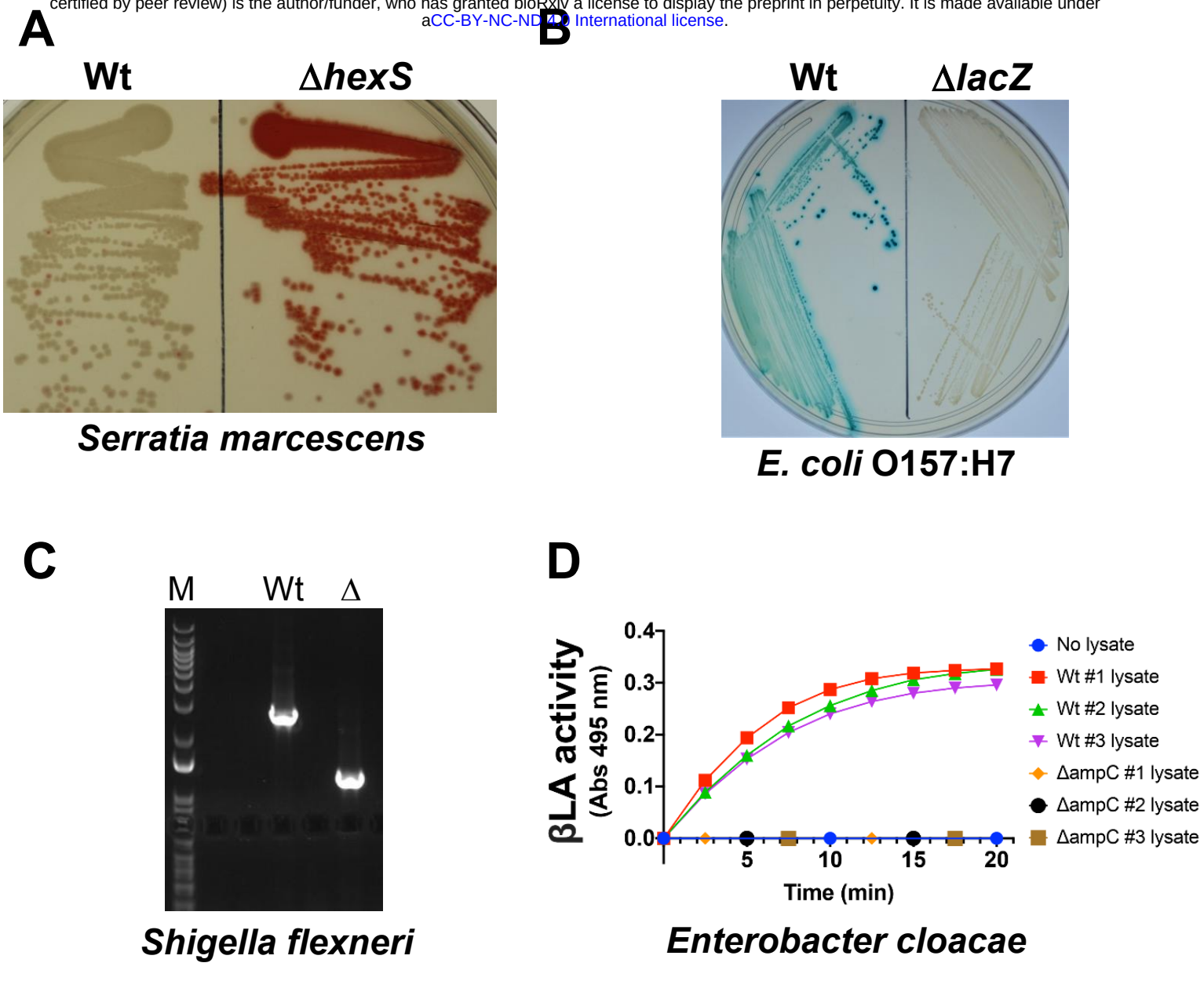

Fig 3 pTOX for genomic modification in multiple pathogens. A) *S. marcescens* colony coloration in Wt (left) *and* Δ*hexS* (right) grown at 37^{O}C for 1 day. HexS inhibits expression of the red prodigiosin characteristic of *S. marcescens.* B) *E. coli* O157:H7 colony coloration in Wt (left) and Δ*lacZ* (right) grown on X-gal-containing media. Blue-green colony color indicates lactose fermentation. C) *S. flexneri* colony PCR and results of 1% agarose gel electrophoresis demonstrating deletion of *ipgH* from *S. flexneri* virulence plasmid. M, marker; Wt, wild-type; Δ, Δ*ipgH*. D) *E. cloacae* beta-lactamase activity in total clarified sonicate from 3 Wt double-crossover colonies and from 3 Δ*ampC* colonies. Sonicates were incubated with nitrocefin, a chromogenic cephalosporin substrate which absorbs at 495 nm when hydrolyzed.

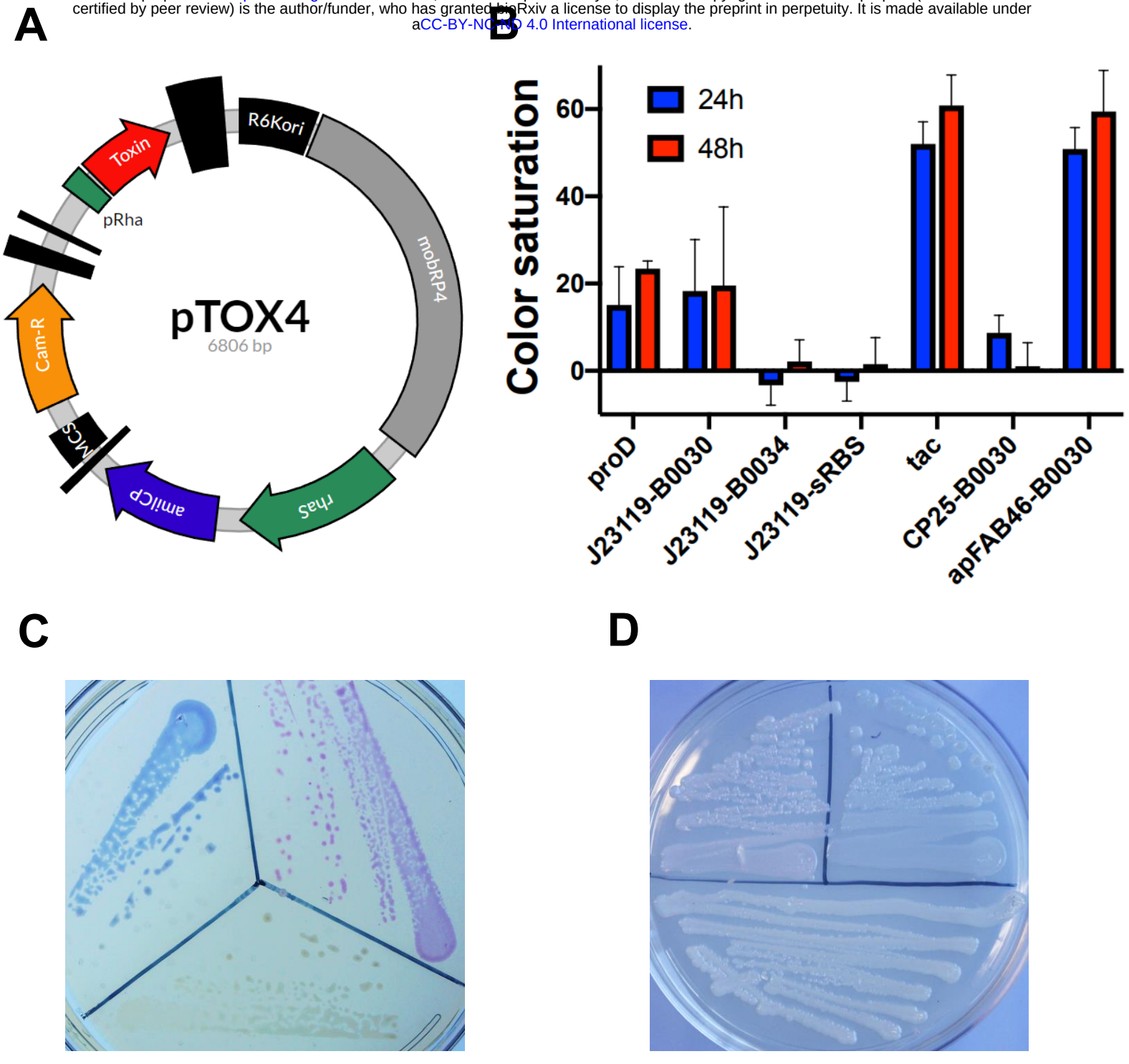

Fig 4 A chromoprotein module facilitates monitoring of conjugation. A) Plasmid map of pTOX4. R6Kori, the R6K origin of replication; mobRP4, mobilization region from RP4 conjugative plasmid; *rhaS*, the rhamnose transcriptional activator; *amilCP*, the blue amilCP chromoprotein; MCS, multiple cloning site; Cam-R, chloramphenicol resistance cassette; pRha, rhamnose promoter. Vertical black bars of varying width represent terminators. B) tac and apFAB46-B0030 allow optimal amilCP expression. Relative color saturation at 24h and at 48h of pTOX4-containing colonies with various promoters and ribosome-binding sites (described in more detail in the Methods). C) Depiction of donor *E. coli* containing (from bottom, clockwise) pTOX without chromoprotein, with tac-*amilCP*, and with apFAB46-B0030-*tsPurple* after 24h at 37^{O}C. D) *E. cloacae* pTOX merodiploids (from bottom, clockwise) without chromoprotein, with tac-*amilCP* , and with apFAB46-B0030-*tsPurple* after 24h at 37^{O}C and an additional 24 hours at 25^{O}C.

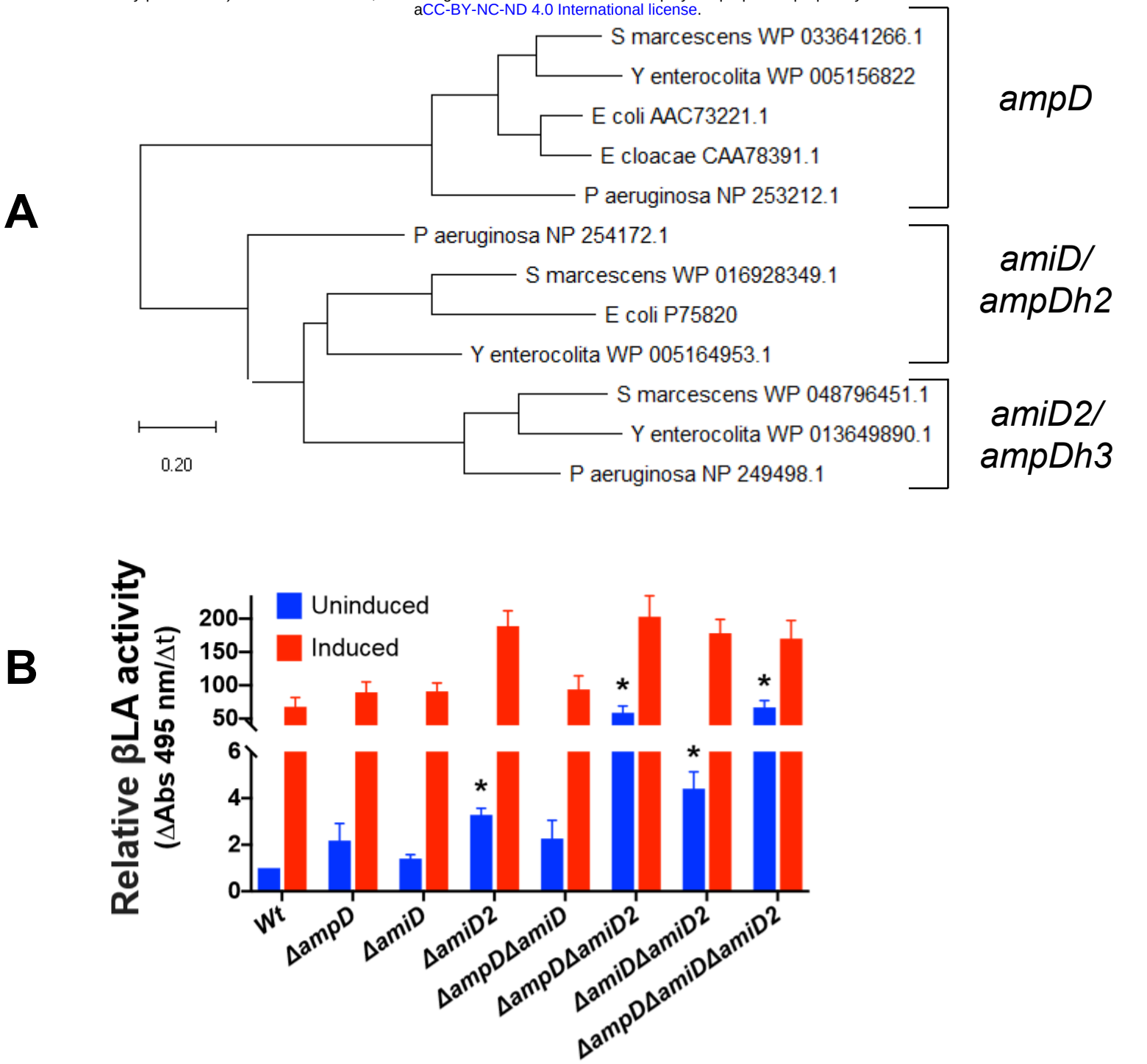

Fig 5 *S. marcescens* peptidoglycan amidohydrolase deletions lead to differential derepression of *ampC.* A) Phylogenetic analysis performed using the Maximum Likelihood method and JTT matrix-based model in MEGA X. An unrooted tree is shown with the lowest log likelihood (-4913). Scale bar = 0.2 substitutions per site. B) Clarified sonicates from indicated strains were incubated with equal amounts of nitrocefin, a chromogenic cephalosporin beta-lactam, and absorbance measured in kinetic mode for 10 minutes. The slope of the line from the first 5 data points were used to calculate beta-lactamase activity, which was then normalized to Wt. Measurements are shown either without pre-induction, and those with induction with cefoxitin 4 µg/mL for 2 hours prior to harvesting. Data represent the mean ± SEM of 4 independent experiments. Comparisons were made between all uninduced mutants and Wt, and between each induced sample and its uninduced control. * = $p < 0.05$ after performing Bonferroni correction. All induced samples are also significantly different from their uninduced samples, except for Δ*ampD*Δ*amiD*, Δ*ampD*Δ*amiD2*, and the triple mutant. These asterisks are not shown for clarity.

		YeaV	MqsR	TseZ
Alphaproteobacteria	Ehrlichia	o	o	o
	Anaplasma	o	o	o
	Wolbachia	o	o	o
	Rickettsia	o	o	o
	Brucella	o	o	o
	Bartonella	o	o	o
Betaproteobacteria	Burkholderia	o	X	o
	Neisseria	X	o	o
	Bordetella	X	X	o
Gammaproteobacteria	Legionella	X	o	o
	Francisella	o	o	o
	Moraxella	o	o	o
	Acinetobacter	o	o	X
	Pseudomonas	o	o	X
	Stenotrophomonas	o	o	o
	Shewanella	o	o	o
	Aeromonas	o	o	o
	Vibrio	o	o	o
	Haemophilus	o	o	o
	Pasteurella	o	o	o
	Hafnia	o	X	o
	Pantoea	X	o	o
	Yersinia	o	X	o
	Serratia	o	o	o
	Klebsiella	X	X	o
	Raoultella	o	o	o
	Enterobacter	X	o	o
	Citrobacter	X	o	o
	Salmonella	X	o	o
	Escherichia	X	X	o
	Shigella	X	X	o
	Proteus	X	o	o
	Morganella	o	o	o
	Providencia	o	o	o
Epsilonproteobacteria	Helicobacter	o	o	o
	Campylobacter	o	o	o

Fig S1 Toxin(s) predicted to be useful (green open circle) in diverse pathogens based on absence of toxin homolog by BLASTP in high confidence genomes deposited in NCBI. Red X's denote presence of toxin gene.

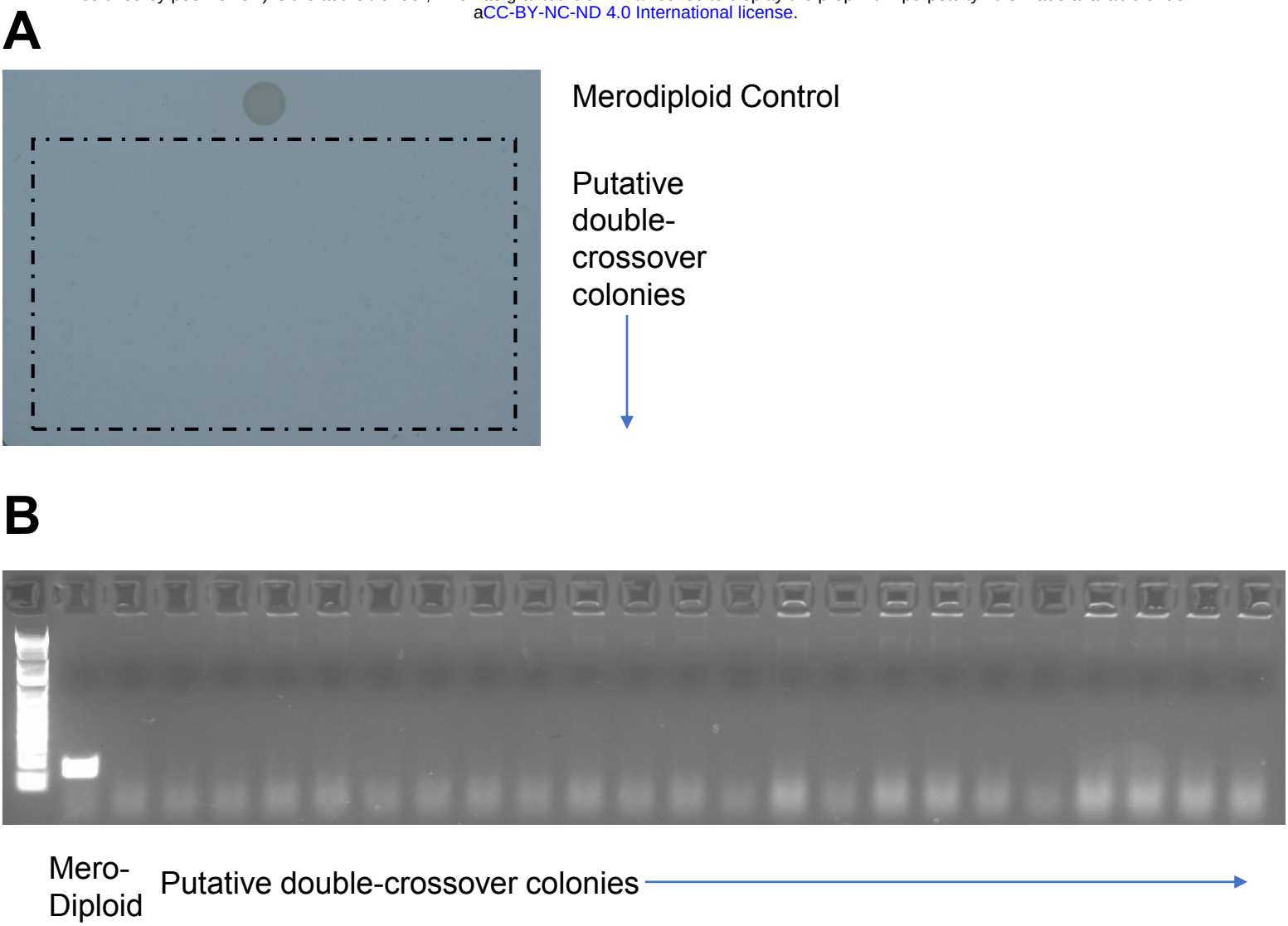

Fig S2 Putative double-crossover *S. marcescens* colonies (for each toxin, 23 colonies from 3 different crossovers) were randomly selected for characterization. Summary results are in Table 1. A) A colony was resuspended in non-selective LB and then spotted onto LB+chloramphenicol. The top colony is the merodiploid positive control. There is no growth where the putative double-crossover colonies were spotted (hatched box). B) Colony PCR was performed for a small intergenic amplicon (between *rhaS* and the chloramphenicol resistance promoter) to test for presence of retained pTOX. The first lane is the merodiploid positive control.

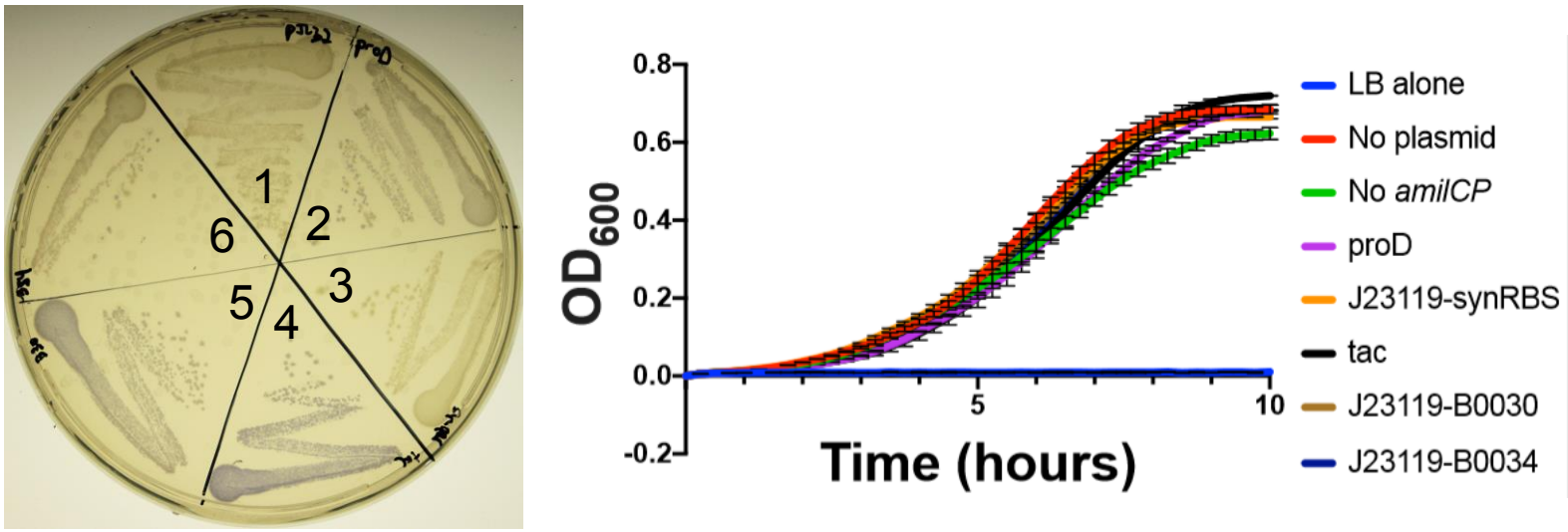

Fig S3 A) *E.* coli donors containing pTOX vectors with *amilCP* and various promoters and ribosome binding sites (RBS) at 24h at 37^{O}C. From top, clockwise: 1) pTOX with no *amilCP;* 2) pTOX-*amilCP* with proD promoter; 3) pTOX-*amilCP* with J23119 promoter and synthetic RBS; 4) pTOX-*amilCP* with tac promoter; 5) and 6) pTOX-*amilCP* with J23119 promoter with the B0030 or B0034 RBS, respectively. B) Growth curves for *E. coli* donor strains (or LB alone) containing pTOX with *amilCP* driven by indicated promoter/RBS.

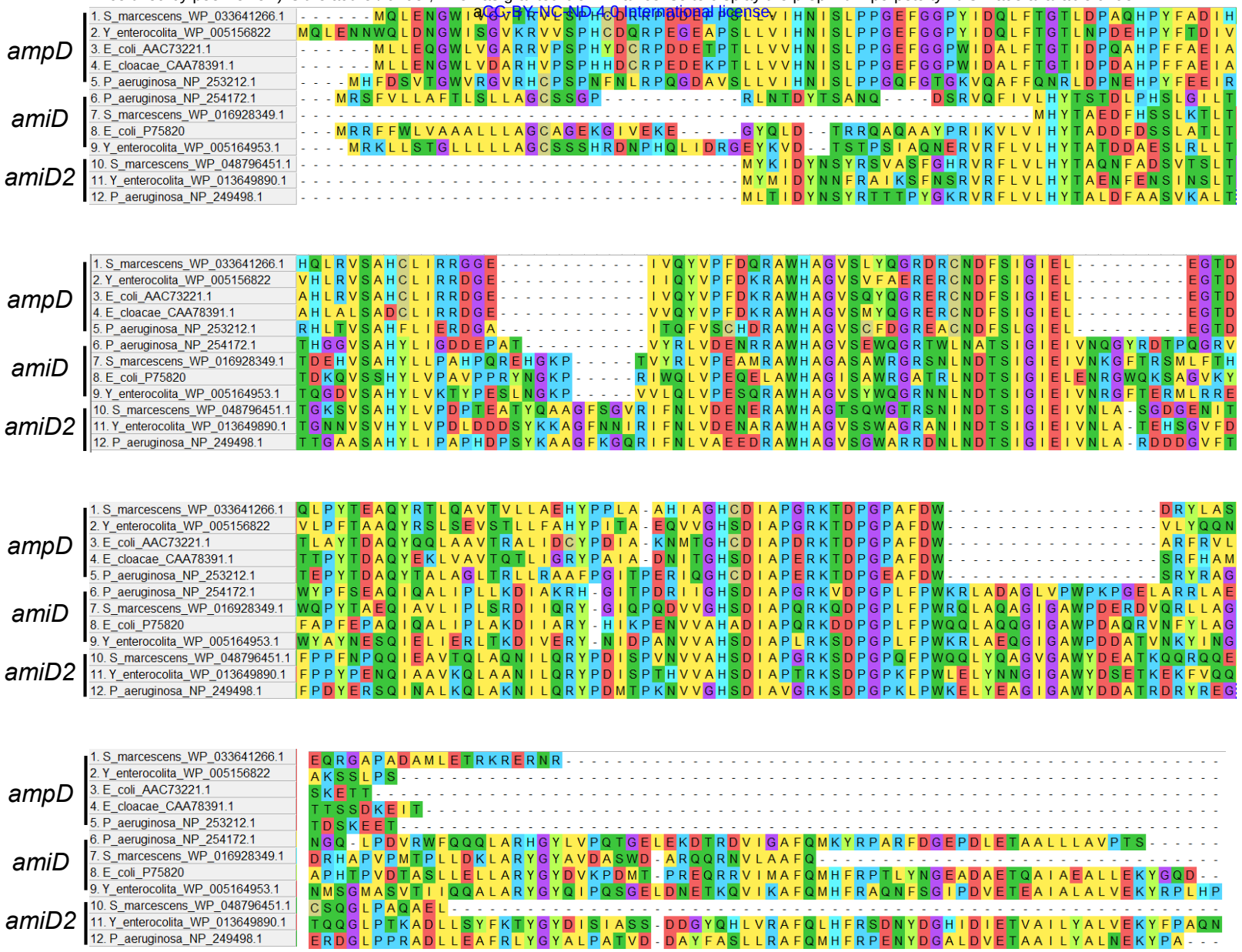

Fig S4 Indicated sequences were aligned in MEGA X using the MUSCLE algorithm (with the UPGMA method). The results are depicted as sequential (reading from left to right from the first through fourth panel) primary sequence.

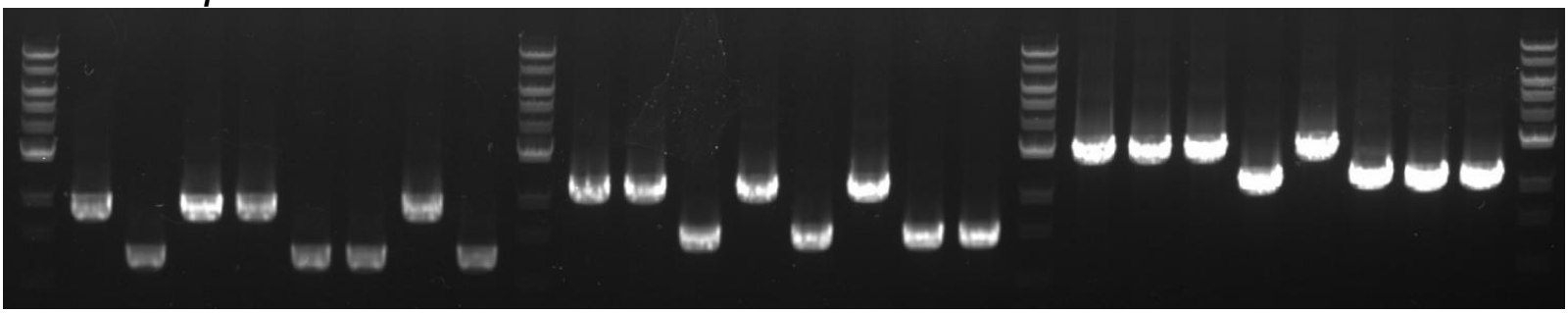

Fig S5 PCR-based genotyping of *S. marcescens* amidohydrolase mutations. Lanes from left to right: marker, Wt, Δ*ampD,* Δ*amiD,* Δ*amiD2,* Δ*ampD*Δ*amiD,* Δ*ampD*Δ*amiD2,* Δ*amiD*Δ*amiD2,* Δ*ampD*Δ*amiD*Δ*amiD2.* The *ampD* locus was amplified with prJL53 and prJL54; *amiD* with prJL55 and prJL56; and *amiD2* with prJL57 and prJL58

Supplemental Text 1

Sequence 1 – Codon-optimized *rhaS* with promoter

cgcggaacccctatttgtttatttttctaaatacattcaaatatgtatccgctcatgagacaataaccctgataaatgcttcaataatattgaa
aaaggaagagtATGACGGTGCTGCACTCGGTTGACTTCTTCCCTAGCGGCAATGCCAGCGTTG
CCATTGAGCCGCGCCTGCCTCAAGCCGACTTCCCGGAGCACCACCACGACTTCCACGAGA
TCGTTATCGTGGAGCACGGTACCGGCATCCACGTTTTCAACGGCCAACCGTACACGATTAC
GGGCGGTACCGTGTGCTTCGTTCGTGATCACGACCGCCACTTATACGAGCACACGGACAA
CTTATGCTTAACCAACGTTTTATACCGTAGCCCTGACCGCTTCCAATTCCTGGCGGGCTTA
AACCAACTGTTACCGCAGGAATTAGACGGCCAATACCCTAGCCATTGGCGTGTGAATCATT
CGGTGCTGCAACAAGTTCGCCAATTAGTGGCGCAAATGGAGCAACAAGAGGGCGAGAACG
ACCTGCCGAGCACGGCGAGCCGTGAAATTCTGTTCATGCAGCTGTTACTGCTGTTACGCA
AGTCGAGCCTGCAAGAAAATTTAGAGAATTCGGCGAGCCGCCTGAATCTGCTGTTAGCGT
GGTTAGAAGATCACTTCGCGGACGAAGTTAACTGGGATGCGGTTGCCGACCAGTTCAGCC
TGAGCTTACGCACCCTGCACCGCCAACTGAAACAACAGACCGGCTTAACCCCGCAACGCT
ATTTAAACCGTTTACGCTTAATGAAGGCGCGCCACTTACTGCGCCATTCGGAAGCGTCGGT
GACCGATATTGCGTACCACTGTGGCTTTTCGGATAGCAATCATTTCAGCACCCTGTTCCGT
CGCGAATTCAATTGGAGCCCTCGCGACATCCGCCAAGGCCGCGACGGTTTCTTACAGTGA

Sequence 2 – Forward terminator and expanded polylinker

AGCTTCGAGCTAATCGcgcaaaaaaccccgcttcggcggggttttttcgcTGATCACGTACGATATCTTCGA
ACCGGTGCACATGGTGTACAGGGCCCTAGGATAGGACGTCTTAAGGTTTAAACCAGGTTA
ATTAATTTAAATGCATCCCGGGACGTCTCGAGCTCGATCGGACCGCGGCCGCTAGCACGT
ATACCAAGTGTCCTGT

Sequence 3 – Synthetic strong ribosome binding site

ttatttttctaaatacattcaaatatgtatccgctcatgagacaataaccctgataaatgcttcaataatattgaaaaaggaGCTTATC
ACCGATAAGGAGGTTTTTTAATGACGGTGCTGCACTCGGTTGACTTCTTCCCTAGCGGCAA
TGCCAGCGTTGCCATTGAGCCGCGCCTGCCTCAAGCCGACTTCCCGGAGCAC

Sequence 4 – *amilCP* with tac promoter

ttgacaattaatcatcggctcgtataatgtgtggaaaggcggttcaccgccgttttcacacaggaaacagaattctttaagaaggagata
tacatATGTCAGTGATAGCAAAGCAGATGACATACAAAGTATATATGAGCGGTACTGTAAATG
GTCACTACTTCGAAGTAGAAGGTGATGGCAAAGGGAAGCCGTATGAGGGTGAACAAACAG
TGAAGCTTACAGTTACGAAGGGTGGCCCTTTGCCGTTCGCGTGGGACATTTTGTCGCCAC
AGTGCCAGTACGGGAGCATACCATTCACCAAGTATCCAGAGGACATACCAGACTACGTGA
AACAGTCCTTTCCCGAAGGCTATACCTGGGAGCGCATAATGAACTTTGAAGACGGTGCGG
TTTGTACGGTATCGAACGATTCATCAATCCAAGGAAATTGCTTTATTTATCATGTTAAATTTT
CGGGGCTTAACTTTCCGCCAAATGGCCCCGTGATGCAGAAGAAAACTCAGGGCTGGGAAC
CAAATACCGAGCGCCTTTTCGCTCGGGACGGAATGCTGTTGGGAAACAATTTTATGGCGTT
GAAGCTGGAAGGGGGTGGCCACTATCTCTGTGAATTCAAGACAACATACAAAGCCAAGAA
GCCTGTCAAGATGCCCGGTTATCACTATGTGGACCGGAAGCTCGATGTCACTAATCACAAC
AAGGATTATACTTCAGTTGAACAGTGCGAAATTTCGATCGCTCGCAAACCTGTCGTAGCAT
AA

Sequence 5 – *tsPurple* with apFAB46 promoter

AGGCCTtctagagtcgacctgcaaaaaagagtattgacttcgcatctttttgtacctataatagattcattactagagaaagaggaga
aatactagATGGCGTCCCTTGTAAAGAAGGATATGTGTGTTAAGATGACAATGGAGGGAACCG
TCAACGGGTATCACTTTAAGTGTGTTGGCGAGGGAGAAGGCAAACCGTTCGAGGGTACAC
AGAATATGCGCATTCGTGTCACCGAAGGGGGCCCTTTGCCCTTTGCTTTCGATATTTTGGC
CCCGTGCTGTATGTATGGTTCGAAGACTTTTATCAAACACGTAAGCGGAATCCCTGACTAC
TTCAAGGAGAGCTTTCCCGAAGGCTTTACTTGGGAACGTACGCAGATTTTTGAAGACGGAG
GAGTTTTGACTGCCCATCAAGATACATCACTTGAGGGAAACTGTTTAATCTACAAAGTTAAG
GTGTTAGGGACAAATTTTCCTGCCAATGGTCCGGTTATGCAGAAAAAGACAGCAGGCTGG
GAACCGTGTGTAGAGATGTTGTACCCCCGCGACGGGGTTCTTTGCGGGCAATCCCTTATG
GCCTTGAAATGTACTGATGGAAATCACTTGACATCCCATTTACGCACCACTTATCGCTCGC
GTAAGCCAAGTAATGCGGTGAACATGCCGGAATTTCACTTCGGAGACCATCGTATTGAAAT
CTTGAAAGCCGAACAAGGAAAATTTTATGAACAATACGAATCCGCAGTGGCACGTTATTCA
GATGTTCCAGAAAAGGCGACTTGATAAggcatgcaagcttggctgtt

Sequence 6 – J23119 promoter with synthetic ribosome binding site

TTGACAGCTAGCTCAGTCCTAGGTATAATGCTAGCTGAGAAAAGAAAGGGAAACTAAGGAG
GTATTTT

SUPPLEMENTAL TABLE 1 Primers used in this study

prAW1	atgcgatatcgagctctcccATGGTGAACATGATGCCGAC
prAW2	TCACACAGGATACAGCTATGTAATAATAACCGGGCAGGCC
prAW3	GGCCTGCCCGGTTATTATTACATAGCTGTATCCTGTGTGA
prAW4	taacaatttgtggaattcccTGCCAACGATCAGATGGCGC
prCJK1	GAGAGGGTACCGCATGCGATATCGAGCTCTCCCGGGTTTTACCCGAAGTCGGGGCG
prCJK2	GCGGATAACAATTTGTGGAATTCCCGATGTATACCCGAATGGCAGCC
prCJK3	TTACTCTTTTTCGAACTCCAGTGAGCGCATATTTAATCCTTCTGTAATAC
prCJK4	GTATTACAGAAGGATTAAATATGCGCTCACTGGAGTTCGAAAAAGAGTAA
prJL1	agactgggcggttttatgga
prJL2	caagatccgcagttcaacct
prJL3	gcttagtacgtactatcaacaggttgaactgcggatcttgcggcaggtatatgtgatggg
prJL4	caattccggttcgcttgctgtccataaaaccgcccagtctacatgtggaattgtgagcgg
prJL5	tgccaataccagtagaaacagacgaagaagTCGTGGCCGGATCCAGCCGA
prJL6	gatcgacgtccccatccagtgcaaagctagattcccgggtcatggctgcg
prJL7	TAAGCAAGATCTctgttgataccgggaagcc
prJL8	tgcttaatcgatgcaacgggaatttgaagacaa
prJL9	gggtgtcggggcgcagccatgaccccgccgacatcataacggttc
prJL10	gcggataacaatttgtggaattcccccacgacttcttcgtctgtt
prJL11	tctagagtcgacctgcaggc
prJL12	ttaccttacttacggcatccgcttacagacaa
prJL13	tttcttgccgccaaggatct
prJL14	catgcgGTACCctctcatcc
prJL15	GCCTCAAGCCGACTTCCCGGAGCACCACCACGACTTCCACGAGAT
prJL16	tcatgagcggatacatatttgaatgtatttagaaaaataaacaaatagggttccgcgAG
prJL17	acagtactgcgatgagtggc
prJL18	agatccttggcggcaagaaa
prJL19	gccctgccactcatcgcagtactgtCGAATCCATGTGGGAGTTTATTCTTG
prJL20	CAAGTGTCCTGTtttcttgccgccaaggatctTTAGGTGGCGGTACTTGGGT
prJL21	accgcatgcgatatcgagctctcccCGGTTAGCGCACCACACTAA
prJL22	CGCCGCGGCGTTATTCTTCTTCGTCCGGACGATTTGCAGTTGTCA
prJL23	CACTATGACAACTGCAAATCGTCCGGACGAAGAAGAATAACGCCG
prJL24	tgagcggataacaatttgtggaattcccAGTTAGTGCGCCACATCGAT
prJL25	accgcatgcgatatcgagctctcccAATGGTGTAATCAAGCCCCT
prJL26	GCCACCCGGCAAAGGTTTACTGTAGCAGTTATCTTCCGTAATAGCGAG
prJL27	GACTCGCTATTACGGAAGATAACTGCTACAGTAAACCTTTGCCGG
prJL28	tgagcggataacaatttgtggaattcccTCGAGGGCGATGACATTGTA
prJL29	accgcatgcgatatcgagctctcccTTTGCGGGTATCGAGCAGGC
prJL30	AACAGCGTAAACAGCGTCATTAGCGCAGACACCTCTCTGCGGTGG
prJL31	AAGTACCACCGCAGAGAGGTGTCTGCGCTAATGACGCTGTTTACG
prJL32	gcggataacaatttgtggaattcccGGTTTGATAGGCGCGCAGAA
prJL33	accgcatgcgatatcgagctctcccGGCGCTGATTTGGTCAGGAT
prJL34	GCAAACTGCACGGCCTGTAACACCAGAAAGCGAATGCGCC
prJL35	GGCGCATTCGCTTTCTGGTGTTACAGGCCGTGCAGTTTGC
prJL36	tgagcggataacaatttgtggaattcccACCCATTTCACCATTCTGCG
prJL37	accgcatgcgatatcgagctctcccTGCTCGTCCTGGTACTCTTC
prJL38	CAGAACGGCGGCGGTTTCGGCATCGTAAAGTCCCTCTCTCGCT
prJL39	AATCAAGCGAGAGAGGGACTTTACGATGCCGAAACCGCCGCCGTT
prJL40	tgagcggataacaatttgtggaattcccCACGATCAGGCTGCGCAGCT
prJL41	GGCTTTCTGCAATAAtcgacctgcattgacagctagctcagtcctaggtataatgctagctactagagattaaagagga gaaatactagATGTCAGTGATAGCAAAGCAGATG
prJL42	GGCTTTCTGCAATAAtcgacctgcattgacagctagctcagtcctaggtataatgctagctactagagaaagaggaga aatactagATGTCAGTGATAGCAAAGCAGATG
prJL43	GGCTTTCTGCAATAAtcgacctgcactttggcagtttattcttgacatgtagtgaggggctggtataatcac atagtactgtttactagagattaaagaggagaaatactagATGTCAGTGATAGCAAAGCAGATG

prJL44	GGCTTTCTGCAATAAtcgacctgcaaaaaagagtattgacttcgcatctttttgtacctataatagattcattactagagatt aaagaggagaaatactagATGTCAGTGATAGCAAAGCAGATG
prJL45	acagcttgtctgtaagcggatgccgtaagtaaggtaaTTGACAGCTAGCTCAGTC
prJL46	TCACTTCTTCGCCTTTTGACACCATAAAATACCTCCTTAGTTTCCCT
prJL47	TCTGTCTAGAttctagagcacagctaacac
prJL48	tcatttgtttagcgatcacactcatctagtactttcctgtgtgac
prJL49	ctagagtcacacaggaaagtactagatgagtgtgatcgctaaaca
prJL50	TCTGTCTAGAttattaggcgaccacaggtt
prJL51	agactgggcggttttatgga
prJL52	ggcttcccggtatcaacagA
prJL53	ATCAGGAAGGCATCGGACAG
prJL54	CTCCAGCGGCGTATTGTG
prJL55	GCCATTTGATCGAGCACGTC
prJL56	TCTCTTCCCCGGCGATCTAT
prJL57	GCTCTGCTACCAGGACGAAG
prJL58	GATCCCCCAACTCTTCCAGC
prJL59	gccaaaacagccaagcttgcatgccTTATGCTACGACAGGTTTGCG

SUPPLEMENTAL TABLE 2 Plasmids used in this study

pDS132	From Phillippe *et al.*
pON.mCherry	From Gebhardt *et al.*
PGR-Blue	From Bradshaw *et al.*
pSB3C5-proD-B0032-E0051	From Davis *et al.*
pSLC-239	From Khetrapal *et al.*
pSLC-241	"
pSLC-246	"
pTOX1	This work. Encodes the YhaV toxin. CAM^R
pTOX2	This work. Encodes the MqsR toxin. CAM^R
pTOX3	This work. Encodes the Tse2 toxin. CAM^R
pTOX4	This work. Encodes the YhaV toxin and *amilCP*. CAM^R
pTOX5	This work. Encodes the MqsR toxin and *amilCP*. CAM^R
pTOX6	This work. Encodes the Tse2 toxin and *amilCP*. CAM^R
pTOX7	This work. Encodes the YhaV toxin and *tsPurple*. CAM^R
pTOX8	This work. Encodes the MqsR toxin and *tsPurple*. CAM^R
pTOX9	This work. Encodes the Tse2 toxin and *tsPurple*. CAM^R
pTOX10	This work. Encodes the YhaV toxin. $Gent^R$
pTOX11	This work. Encodes the MqsR toxin. $Gent^R$
pTOX12	This work. Encodes the Tse2 toxin. $Gent^R$